JOURNAL OF MATERIALS SCIENCE 31 (1996) 4967-4973

Duralumin–stainless steel joint: structure and mechanism of forming by means of electron beam welding and Ag–2Mg filler metal shim

A. GRODZINSKI*, J. SENKARA‡,*, M. KOZLOWSKI*
*Institute of Vacuum Technology, 44/50 Dluga St., 00-241 Warsaw, Poland and ‡Warsaw University of Technology, Welding Department, 85 Narbutta St., 02-524 Warsaw, Poland

High-alloyed stainless steel of 18–8 type and duralumin are not directly weldable due to significant differences in their properties. The results of structural investigations of the joints between the two materials, obtained by a previously developed method of electron beam welding with an Ag–2 wt% Mg alloy filler metal shim, are presented in this paper. The microstructure of the weld is diphasic, being composed of supersaturated Ag in Al solid solution and also an Ag_2Al phase. At the base materials and weld boundaries interstitial layers are crystallized in the form of solid solutions while brittle intermetallic compounds do not appear. On the basis of presented results a mechanism for the joint formation is proposed.

1. Introduction

Thermally treated aluminium alloys and stainless steel form an interesting couple from the point of view of application in vacuum technology. However, such materials can not be directly welded due to large differences in their physical properties (particularly the fusion points and thermal expansion coefficients). In addition a brittle Al–Fe intermetallic compound forms during the welding process [1]. Significant difficulties also arise due to; (a) the tendency of aluminium alloys to hot cracking (b) the vapourization of some alloying elements with high vapour pressure (e.g. Mg, Zn) and (c) damage to the dispersion hardened structure in the heat affected zone, all of which result in a decrease of the joint strength.

In a recent work [2] results have been presented on the production of welds between high alloyed chromium–nickel 18–8 type stainless steel and duralumin. These welds were produced by means of electron beam (EB) welding with an especially chosen filler metal, a shim made of Ag–2 wt % Mg alloy, which has metallurgical compatibility to both base materials. Faultless welded joints with satisfactory properties were obtained by the method. Selected features, such as tensile strength, impact strength and vacuum tightness, were measured in relation to the EB welding parameters. Initial results of a structural analysis were also presented. Because the EB was directed onto the edge of the stainless steel during welding, numerous macroscopic particles of the material were found in the welds as a result of the carrying and dispersing of steel droplets in the bulk due to intensive movement of the liquid pool. Such a joint design promotes a reduction in the residual stresses which are responsible for cracks in the welds between two materials with a large mismatch in the thermal expansion coefficients.

The aim of the present study is an investigation of the microstructure of the welds obtained by the developed method with a special interest in the interphase boundaries between the weld and both base materials. In addition we will present a discussion on the formation mechanism of such joints.

2. Experimental procedure

2.1. Materials and sample preparation

1H18N9T type stainless steel according to Polish standards (corresponded to 321 steel acc. ASTM) and PA6 type duralumin (approximated 2024 alloy acc. ASTM) were used in the welding experiments. Both materials were used in the form of a 6 mm thick sheet. In turn, a 0.15 mm thick foil made of Ag–2 wt % Mg alloy was used as a filler metal shim. The chemical composition of all materials, examined by the atomic absorption spectrometry (AAS), is presented in Table I.

The stainless steel acquires the typical structure of carbon supersaturated austenite with 5% δ ferrite. Duralumin was applied in a heat treatable state. For this purpose the material was annealed for 18 h at 500 °C, cooled in cold (5 °C) water and spontaneously aged for 100 h. The precipitation hardening effect was monitored by microhardness measurements. As a result of such a heat treatment, a material with a dispersion hardened structure was obtained. The Ag–2 wt % Mg foil has the structure of the α limited solid solution.

0022–2461

TABLE I Chemical composition of used materials. The data was determined using the atomic absorption method (AAS)

Material	C wt %	Mn wt %	Cr wt %	Ni wt %	Ti wt %	Cu wt %	Mg wt %	Zn wt %	Al wt %	Fe wt %	Ag wt %
Stainless steel 1H18N9T	0.1	1.6	17.3	8.7	0.4	–	–	–	–	bal.	–
Duralumin PA6	–	0.6	–	0.1	0.1	4.5	0.4	0.1	bal.	0.4	–
Filler metal Ag–2Mg	–	–	–	–	–	–	2.0	–	–	–	bal.

The base materials with filler metal shim were EB welded with the parameters for which the best results were previously achieved [2]. These are a 30 kV accelerating voltage, a beam current of 30 mA and a welding speed of 50 cm min^{-1}, at a pressure of 10^{-2} Pa in the vacuum chamber. The EB was directed onto the edge of the steel sample and oscillated. A schematic illustration of the process is presented in Fig. 1.

The structure of the joints was analysed using optical and electron microscopy techniques (SEM, TEM), X-ray microanalysis (EPMA) and the phase analysis was probed using X-ray diffraction (XRD). An automatic television image analyser was used for quantitative structure measurements. Specimens for the majority of the tests were prepared in the usual way by producing a metallographic section perpendicular to the joint axis. Samples for TEM were turned on a lathe from a 3 mm diameter rod which was cut into 0.1 mm thick slices and then ion thinned. Powder samples for XRD were prepared by introducing a notch along the face of the weld in its symmetry plane which was then fractured allowing mechanical removal of succeeding layers from the centre to the fusion lines.

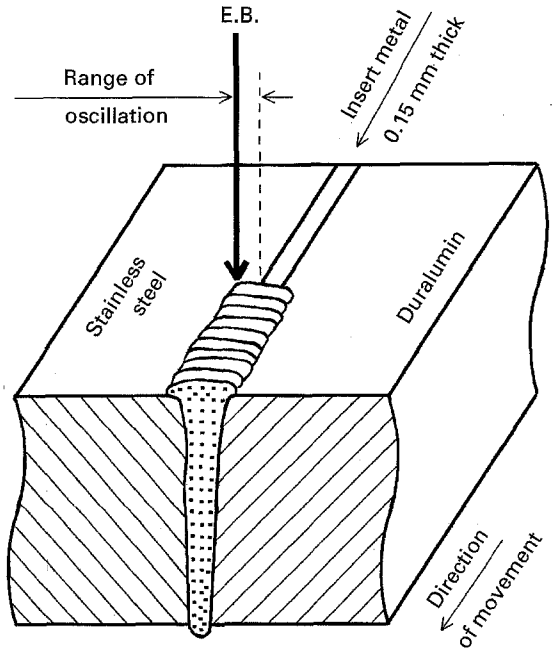

Figure 1 The principle of EB welding of stainless steel with duralumin by the use of a Ag–2 wt % Mg filler metal shim.

3. Results

3.1. The middle of the joint

The macroscopic construction of the joint is presented in Fig. 2. The weld is constituted of filler material mixed in the liquid state during welding with both the base materials. It is evident from the figure that the partially molten edges and the width of the weld are significantly higher than the width of the applied filler metal shim. Numerous steel inclusions are visible in the weld which is, as was previously mentioned, an effect of directing the EB onto the edge of the base material.

A typical microstructure in the middle of the joint is presented in Fig. 3a and the surface distribution of the main elements: Ag, Al and Fe are also shown in Fig. 3 (b–d). It is clearly seen from the pictures that the weld is built of two phases, a light and a dark one, which are composed of Ag and Al. Quantitative point microanalysis shows a changeable chemical composition of the mentioned phases over a fairly wide concentration range of the order of 10 wt %. Ag dominates in the light phase whereas the weight relation of the two elements in the dark phase is nearly 1:1. A small amount of copper, on the order of 1 wt %, is revealed in both phases. Detailed results of the microanalysis are collected in Table II.

In certain regions the existence of dissolved Fe was distinguished and their microstructural constitution is different to the other ones (see Fig. 3(a, b)). From this observation, it can be concluded that Fe plays the role

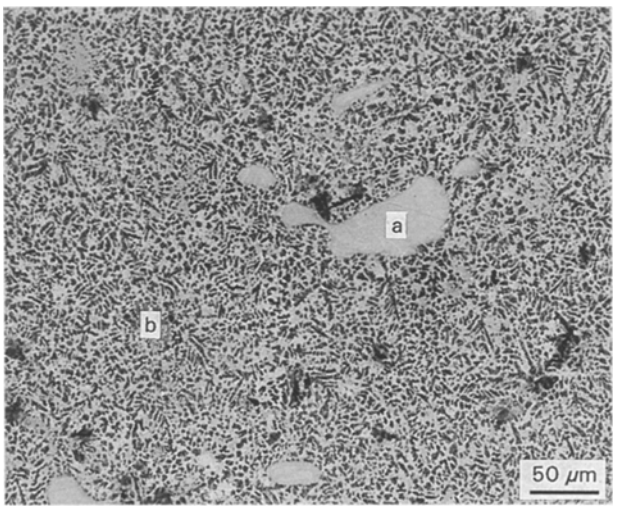

Figure 2 Macrostructure of the joint. Irregular steel particles (a) are dispersed in the weld (b).

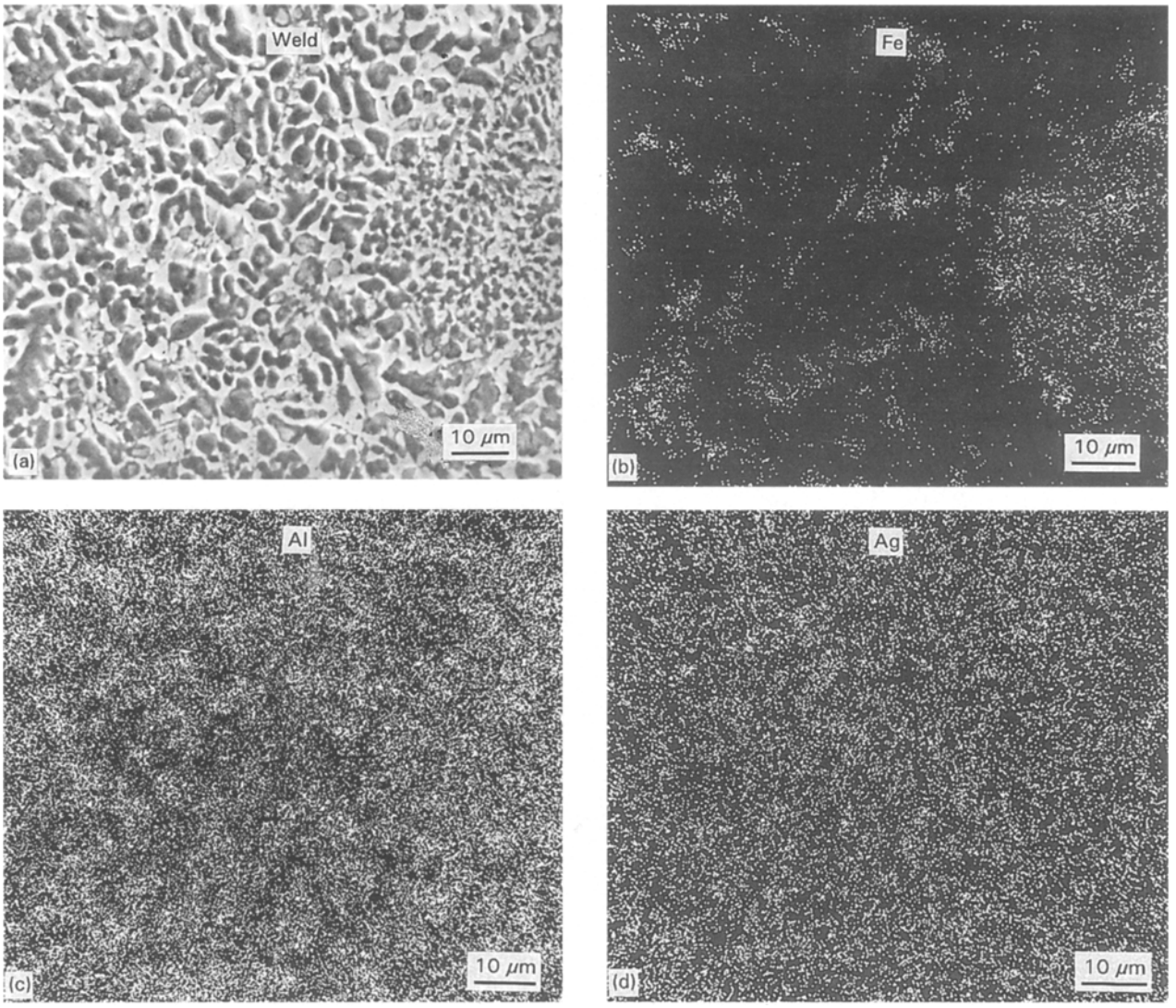

Figure 3 Microstructure in the middle of the joint: a – secondary electron image (SEI), b–d – distribution of the main elements.

TABLE II The phase composition of the welds (see Fig. 3a) as determined on the basis of EPMA, TV image analyser, and XRD techniques

Phase	Chemical composition wt %			Phase content [vol %]	Lattice type	Lattice parameter 10^{-10} m	Identification
	Ag	Al	Cu				
light	65.5–73.9	33.3–24.8	ca 1.0	26.7 ± 2.6	A3 (hex)	2.880; 4.620	δ (Ag_2Al)
dark	47.2–54.6	51.0–43.8	ca 1.0	balance	A1 (fcc)	4.046–4.048	Ag(Al)

of a modifier of the crystallization causing grain refinement. The remaining alloying elements in the steel, such as Cr, Mn and Ni, the distribution of which is not presented in the paper, accompany Fe. It did not prove possible, to obtain by the used EPMA method, any information about the presence and distribution of carbon and magnesium that could occur in small amounts in the joint. The quantitative structure measurement using the television image analyser showed that the total surface covered by the light phase in Fig. 3a was approximately 26%. Taking into account the Cavalieri–Acker principle we assume the same volume contribution of this phase in the joint.

Fig. 4 presents a diffraction pattern of the material from the middle of the joint. All the diffraction peaks that could be indexed showed that the Ag_2Al, Al and Fe phases were present. The threshold for the detection of phase existence was estimated for this case as 1% of the volume fraction. The shape of the "peaks" suggests the existence of solutions or residual stresses. Calculated lattice parameters (see Table II) differ slightly, in the range of measurement error, from the values which are characteristic for pure phases. This does not exclude, however, the existence of Ag–Al solutions which are possible if the insignificant difference in the Ag and Al atom size are considered. Similar phase composition results have been observed for

powder samples taken from the middle of the joint towards steel and also towards duralumin.

The investigations made by the use of a high resolution JEM 2000EX transmission microscope confirmed the existence of the two areas observed as light and dark regions in the SEM (Fig. 3a). Electron diffraction was applied to identify the phases in these areas. The TEM results corroborated the conclusions of the EPMA and XRD work. In addition, the method revealed that a AlFe phase occured in the weld at concentrations below the sensitivity threshold of the XRD technique.

A TEM micrograph of the region of the joint in which the existence of dissolved Fe was observed (see Fig. 3b), is shown in Fig. 5. The electron diffraction experiments showed that in addition to the δ Ag_2Al phase with an hexagonal symmetry and lattice parameters listed in Table II, there existed an AlFe intermetallic compound which had a cubic symmetry and a lattice parameter of 2.895×10^{-10} m. It is created as a result of ordering of an α Fe solid solution [4].

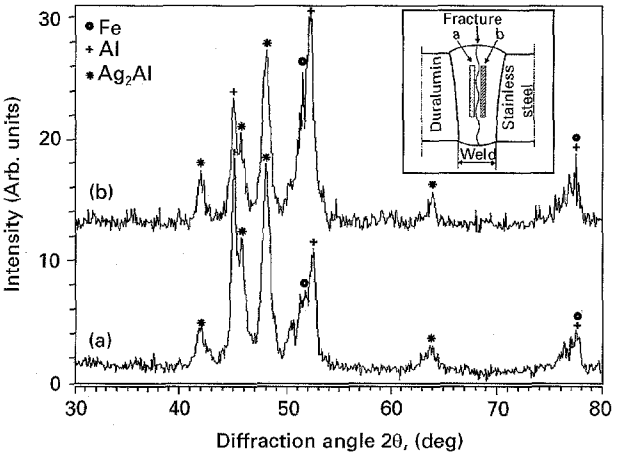

Figure 4 Diffraction pattern of powdered material from the middle of the joint with (a) showing the duralumin side and (b) the steel side.

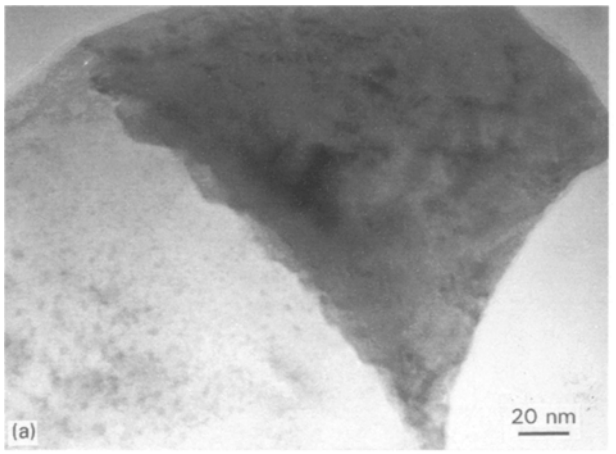

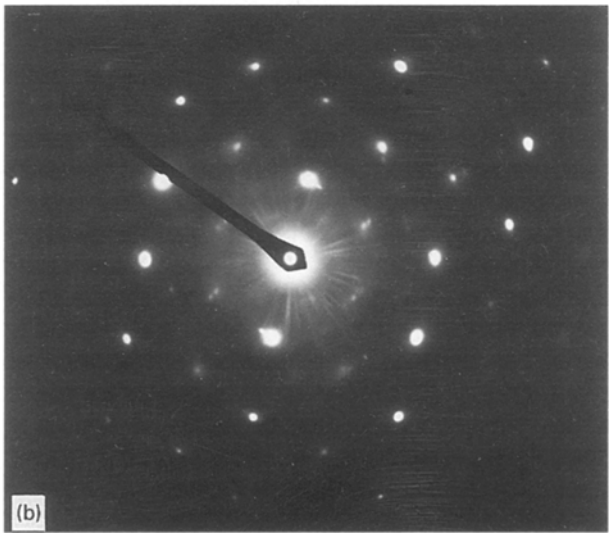

3.2. Duralumin – weld interface

The area around a boundary (fusion line) between base material and a weld is an important place whose structure often determines the quality and strength of a joint. Most welding defects also appear in this region.

The analysis of a duralumin – weld boundary revealed the existence of the dark phase, rich in Al, in the form of a layer close to this interface, on the weld side (Fig. 6). Concentration profiles perpendicular to the fusion line for the elements (not reported in this paper) show that it is a solution of Ag in Al with changeable composition.

A penetration of Ag along duralumin grain boundaries is also visible at a distance of 80 μm. A schematic illustration of the grain boundary penetration by the liquid is shown in Fig. 7a. Inclusions of an Ag-rich phase are formed at grain boundaries of the base material in the zone adjoining the fusion line as an effect of this penetration. The measurements of the angles formed between the boundaries of the inclusions were carried out by metallographic cross-sections. They correspond to the dihedral wetting angles of duralumin by the liquid during welding. The results of 250 measurements are presented in the form of a histogram in Fig. 7b. The "true" value of the dihedral wetting angle, calculated by statistical techniques is 13°. It should be added, however that the conditions

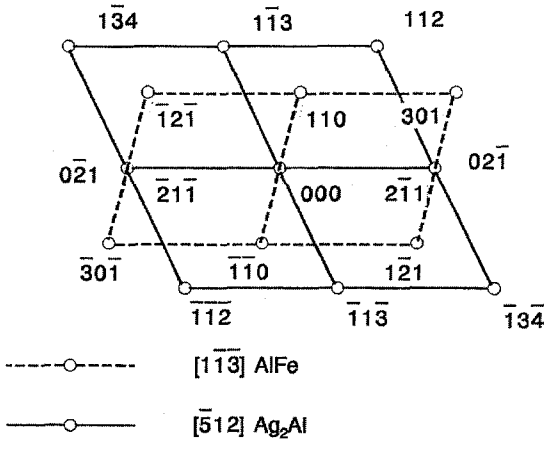

Figure 5 (a) TEM micrograph and (b) electron diffraction pattern of AlFe phase in the region in the weld where Fe was dissolved.

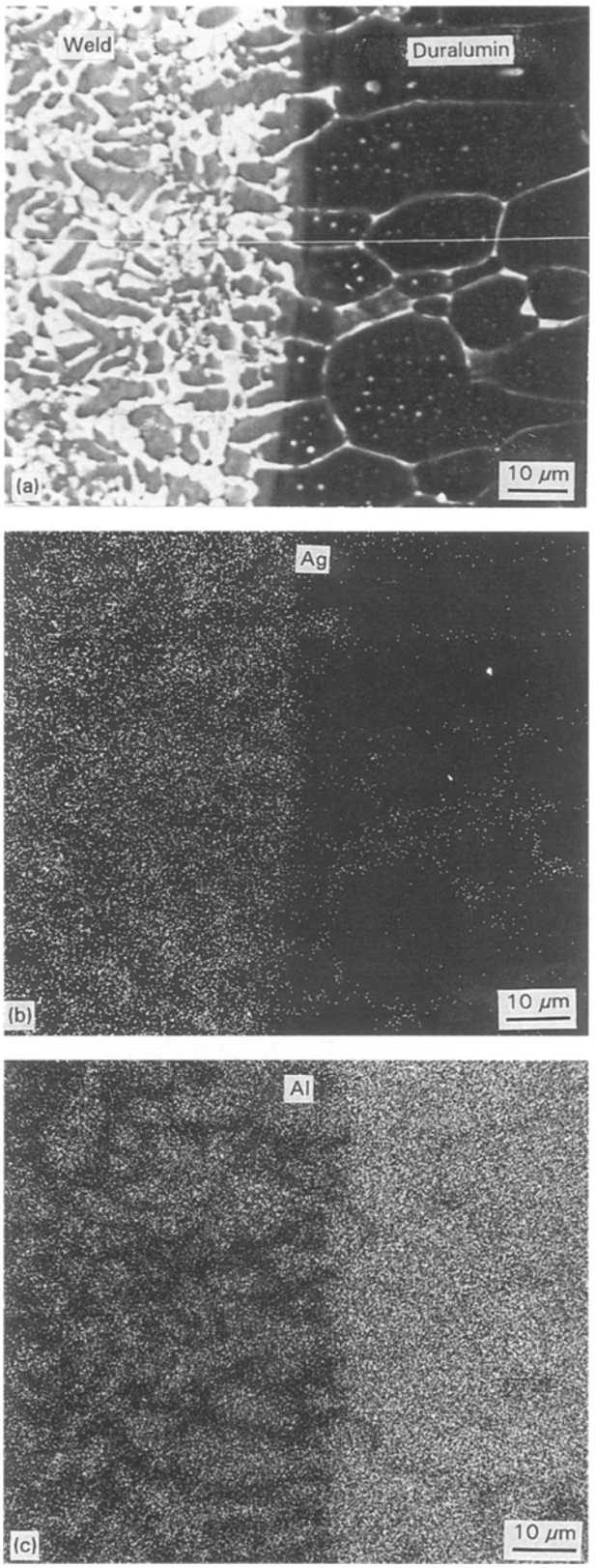

Figure 6 Duralumin – weld boundary: (a) SEI, (b), (c) distribution maps of Ag and Al.

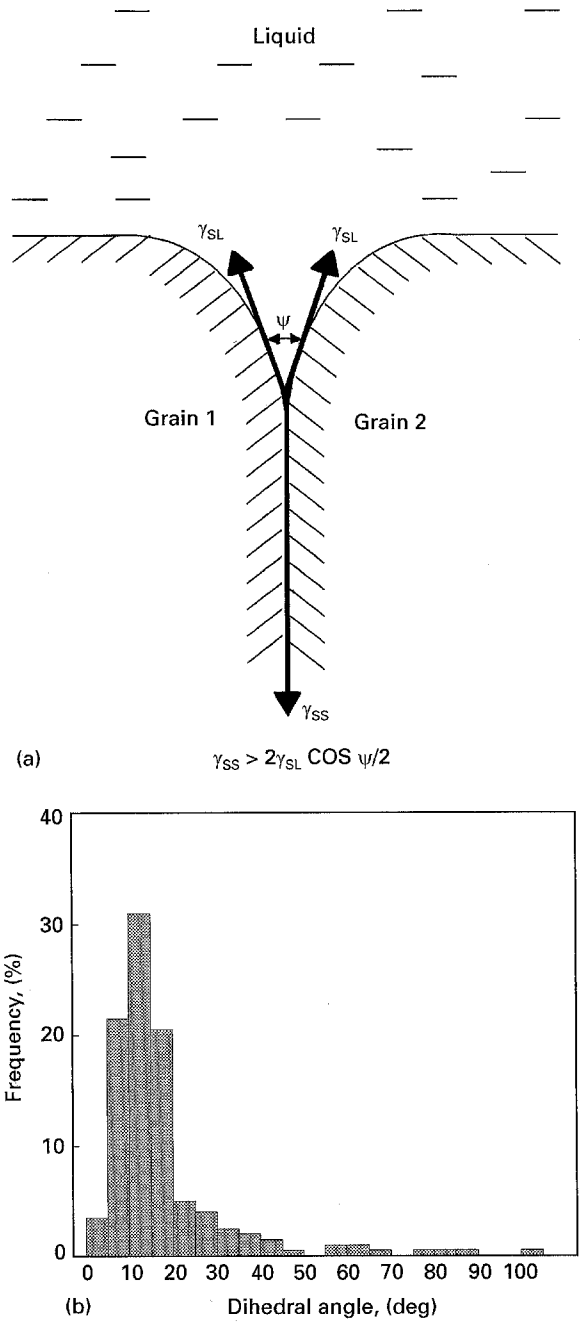

Figure 7 Dihedral wetting angle ψ between the liquid and solid phases: (a) the scheme and condition of penetration along grain boundary (γ_{SS} and γ_{SL} are solid–solid and solid–liquid interfacial tensions, respectively), (b) statistical distribution of the 250 measurements.

for forming a dihedral angle significantly differ from the equilibrium ones. Moreover, the penetrating liquid was at a higher temperature than the melting point of the base material (duralumin). Thus it is possible that the appearence of such a configuration was connected with the occurrence of an abrupt temperature gradient and short contact time of the liquid with the solid.

The diffraction pattern of the weld material close to the boundary with the duralumin is presented in Fig. 8. The reflections of high intensity originate from Ag_2Al and Al phases. In addition much less intense reflections from Fe, are visible. The comparison of XRD and EPMA results (Fig. 6) confirms the existence of Ag in Al solid solution and an Ag_2Al phase near the fusion line.

3.3. Stainless steel – weld interface

The continuous grey coloured interstitial layer which crystallized at the weld–stainless steel boundary was identified as the solid solution of Al in Fe (Figs 8 and 9). In the diffraction pattern the highest relative

intensity peak is due to this phase. The remaining diffraction lines may be attributed to the Ag_2Al phase and to solid solution of Ag in Al. The intermetallic compounds, that are known to occurr in the Al–Fe phase equilibrium diagram [3] such as Fe_3Al, FeAl, $FeAl_2$, Fe_2Al_5, $FeAl_3$, were not observed.

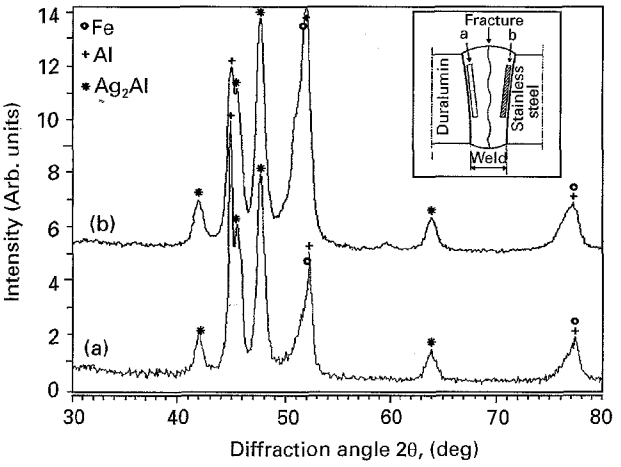

Figure 8 Diffraction pattern of powdered material from the area around the fusion line in duralumin and steel. (a) The pattern was taken on the duralumin side and the (b) pattern on the steel side of the weld.

4. Discussion

4.1. Mechanism of formation of the joint

Discussion of the above mentioned results on the structural investigations of the welded material and the area around both fusion lines allows us to propose a mechanism of creation of the joint between stainless steel and duralumin by the use of a Ag–2 wt % Mg filler metal shim.

Under the action of the EB, the filler material melts and so does a part of the adjoining duralumin. A liquid solution forms which is initially composed of metals Ag and Al whose melting points are lower than the melting point of steel.

The EB spot on the steel surface is oscillating which causes intensive stirring of the molten bead thus macroscopic steel particles are separated from the base material and dispersed in to the liquid. They begin to dissolve in to the melt but on account of the short time of contact (connected with the relative high welding rate) only the smallest have a chance to completely dissolve.

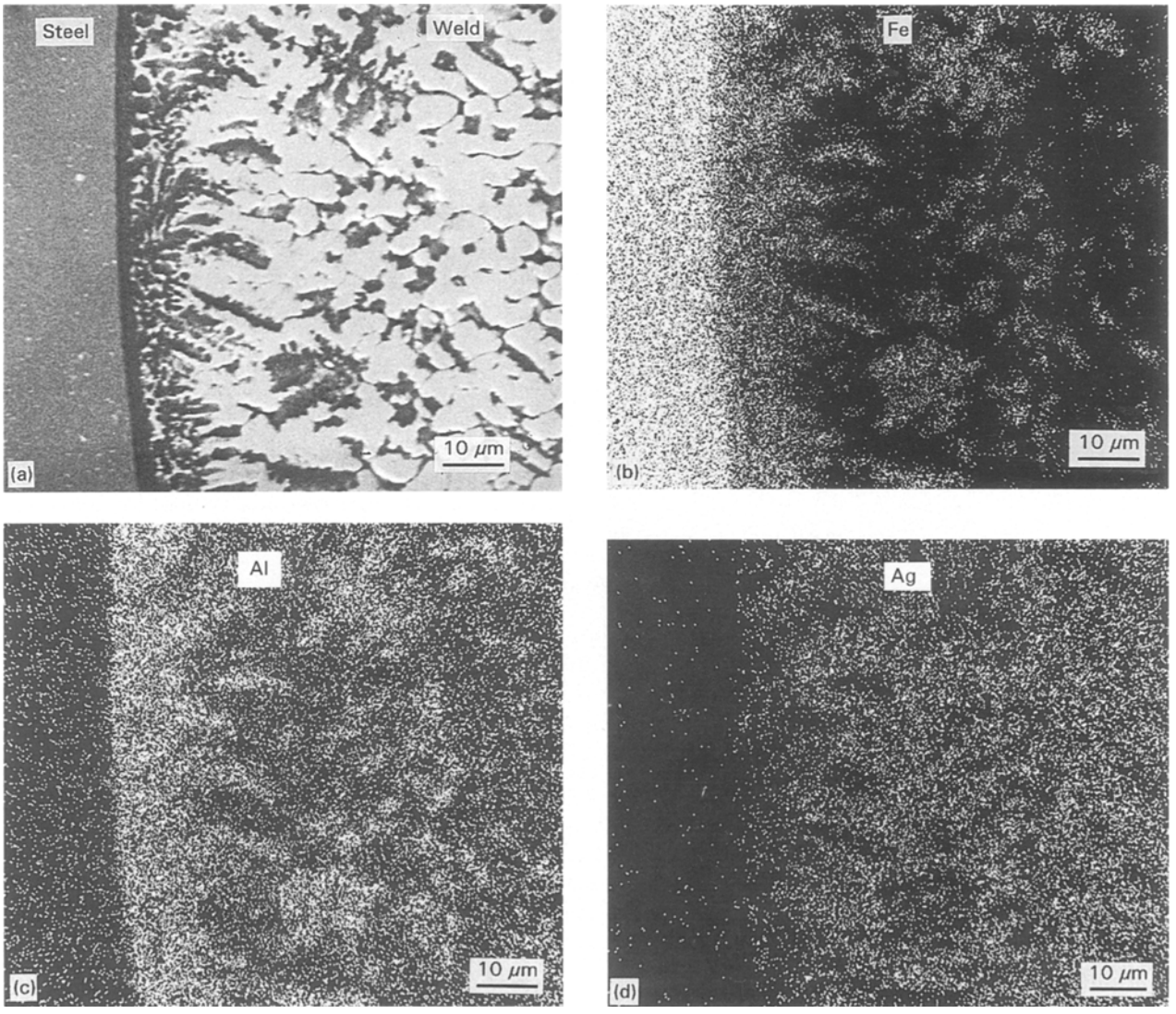

Figure 9 Stainless steel – weld boundary: (a) SEI, (b)–(d) – distribution of elements.

There is a reason for the presence of Fe and accompanying alloying elements (Cr, Ni, Mn) being detected in only some regions of the weld. The liquid solution also dissolves in the vicinity of the grain boundaries in duralumin followed by penetration into the material. This penetration is possible due to an advantageous relationship between the interfacial tensions which allows the formation of an acute dihedral wetting angle. The depth of penetration is undoubtedly connected with the temperature gradient and the time of interaction between the liquid and solid phases.

A crystallization process starts after the translocation of the heat source. It is of heterogeneous character: partially melted grains of the base material serve as the nuclei, which is clearly visible in Fig. 6a. The direction of crystallization is opposite to the heat flow, from the fusion line to the middle of the joint. A characteristic multi-phase joint structure forms with these macroscopic steel particles that did not have enough time to dissolve (Fig. 2).

A layer of Ag(Al) solution crystallizes at the fusion line of duralumin whereas at the border of steel a layer of Al(Fe) solution which may have a wide range of concentration crystallizes [3]. However, Al–Fe intermetallic phases are not created in any significant concentrations, neither as a result of direct crystallization from the liquid nor due to possible ordering and segregation of a Fe-rich solid solution [4]. This is perhaps an effect of the fast cooling ratio. The formation of continuous layers of solid solutions at the interfaces instead of brittle intermetallic compounds secures high adhesion of the joint and its other satisfactory features, notably a lack of cracks. Moreover, the presence of dispersed, macroscopic steel particles decreases the level of residual stresses in the weld [2].

The structure of the weld is diphasic. A basic chemical composition of a liquid bead during welding, estimated on the basis of quantitative measurements of volume contribution of phases (see Table II), suggested a composition of Ag–41.5 wt % Al. Due to lack of data concerning the densities of the Ag(Al) solution and Ag_2Al phase, we applied a simplifying assumption concerning a linear relationship between the densities and the Ag/Al ratio. On this basis the densities were calculated to be 6.85 and 8.15 $g\,cm^{-3}$ respectively.

The course of the crystallization may be discussed in the light of the Ag–Al phase diagram reported in [3]. In near equilibrium conditions, the solution on the Al base should crystallize first followed by an δ (Al) eutectic. The dark phase distinguished in the weld (Fig. 3) was identified as a supersaturated Ag in Al solid solution with a high Ag content (Figs 4 and 5; Table II). Such a high Ag concentration in the phase testifies to the high cooling ratio of the joint since the microstructure was effectively "frozen" due to the rapid heat removal. However, structural investigations did not find the expected eutectic because a second light phase was revealed which proved to be a secondary solution based on the Ag_2Al compound (Figs 4, 5; Table II) but with a far from stoichiometric composition. This is also an effect of the quick, "non-equilibrium" crystallization.

The Fe dissolved in certain regions of the weld plays the role of a structural modifier causing grain refinement. A localised α Fe solid solution orders forming the small amount of AlFe phase distinguished by electron diffraction (Fig. 5). Because of the insignificant fraction of this intermetallic compound (< 1 vol %), its presence should have no disadvantageous influence on the macroscopic properties of the joint. This was observed in practice [2].

5. Conclusions

(1) As a result of EB welding of high-alloyed, chromium–nickel stainless steel with duralumin using Ag–2 wt % Mg filler metal shim, good welds with a complicated structure were obtained.

(2) Interstitial layers of Ag(Al) and Al(Fe) solid solutions without any of the brittle intermetallic compounds that exist in the Al–Fe equilibrium phase diagram, are created at the fusion lines of the weld. The solid solution layers are responsible for the excellent properties of the joint.

(3) An Ag(Al) solid solution and an Ag_2Al phase with a non-equilibrium composition compose the base of the weld. Additionally, a small amount (< 1 vol %) of an AlFe intermetallic compound was revealed.

(4) The effect of a liquid phase penetration into the duralumin in addition to a modification of the crystallization process by dissolved Fe, were observed.

(5) The complicated and non-equilibrium structure of the joints is partially the result of multiple chemical composition and partially due to the fast cooling ratio of the material which is characteristic of the deep, narrow welds obtained by EB welding.

Acknowledgement

This work was sponsored by the Polish Committee for Scientific Research.

References

1. "*Welding Handbook*", 8th edn, (American Welding Society, Miami Fl., 1991).
2. A. GRODZIŃSKI and J. SENKARA, *Metals Alloys Technologies*, **3–4** (1995) 385.
3. T. B. MASSALSKI, "*Binary alloy phase diagrams*", 2nd edn, (American Society for Metals, Metals Park, OH, 1990).
4. M. HASAKA, *Trans. Jap. Inst. Met.* **21** (1980) 660.

Received 7 July 1994
and accepted 15 December 1995